Materials Physics and Mechanics. 2023;51(7): 15-21
Research article
http://dx.doi.org/10.18149/MPM.5172023_3

Submitted: January 11, 2023
Approved: March20, 2023
Accepted: November 24, 2023

Synthesis and characterization of iron-doped TiO_2 nanotubes for dye-sensitized solar cells

B. Samran [1], E.N. Timah [2], P. Thongpanit [1], S. Chaiwichian [3] ✉

[1] Nakhon Phanom University, Nakhon Phanom, Thailand

[2] Trinity International School, Bangkok, Thailand

[3] Rajamangala University of Technology Isan Sakonnakhon Campus, Sakonnakhon, Thailand

✉ saranyou530531117@gmail.com

Abstract. Titanium dioxide nanotubes as materials for energy conversion were successfully synthesized, characterized and tested for dye-sensitized solar cells (DSSC). The TiO_2 nanotubes were grown by one face anodization at room temperature on titanium sheets of 0.25 mm thickness and 99.7 % purity. The electrolyte was composed of ethylene glycol, ammonium fluoride (0.3 wt. % NH_4F), deionized water (2 vol. % deionized water) and $Fe(NO_3)_3$ as dopant source with varying concentrations of 2, 4, 6 and 10 mM. The X-ray diffraction (XRD), scanning electron microscopy (SEM), atomic force microscopy (AFM) and ultraviolet–visible spectrometry (UV-vis) techniques were used to characterize the TiO_2nanotubes. Finally, the samples were tested in dye-sensitized solar cells and their conversion efficiencies were calculated. According to the results, amorphous TiO_2 was transformed into the crystalline anatase phase after heat treatment. Under the given experimental conditions, our optimal results were obtained for the titanium dioxide nanotubes (TNTs) at 6 mM of iron (III) nitrate. The maximum DSSC conversion efficiency was 4.66 % for the TNTs of 6 mM $Fe(NO_3)_3$. The findings of this research provide significant guidelines for current and future research in the development of renewable energy.
Keywords: renewable energy; dye-sensitized solar cells; TiO_2 nanotubes; iron (III) nitrate

Acknowledgements. *The authors would like to greatly thank the Thailand Science Research and Innovation, Fundamental Fund: FF 2022, the Division of Physics, Faculty of Science, Nakhon Phanom University, Muang District, Nakhon Phanom and Faculty of Industry and Technology, Rajamangala University of Technology Isan for support.*

Citation: Samran B, Timah EN, Thongpanit P, Chaiwichian S. Synthesis and characterization of iron-doped TiO_2 nanotubes for dye-sensitized solar cells. *Materials Physics and Mechanics*. 2023;51(7): 15-21. DOI: 10.18149/MPM.5172023_3.

Introduction

The first dye-sensitized solar cells (DSSCs) were fabricated by O'Regan and Gratzel [1]. As a renewable sources of energy, DSSCs have several advantages such as low production cost, simple preparation method and relatively high efficiency [2]. Titanium dioxide (TiO_2) has semiconducting properties, which has attracted its usage in solar cell fabrication. Titanium dioxide has several other beneficial properties such as low toxicity, high photocatalytic activity, resistance to corrosion, excellent dielectric effect, chemical stability, availability and low cost. These amazing properties have made TiO_2 to have a wide range of applications such as in gas sensing, photocatalysis, hydrogen generation, photovoltaic, and water purification [3–5].

Publisher: Peter the Great St. Petersburg Polytechnic University

The use of titanium dioxide nanotubes (TNT) in solar cells and photocatalysis has grown of recent due to the benefits of slower rates of charge recombination and higher efficiencies [6–9]. To overcome the large energy band gap (3.2 eV) of titanium dioxide (TiO_2), doping with foreign elements has been employed successfully [10]. In 2009, Dholam and Patel reported the use of sputtering and sol-gel techniques to dope TiO_2 nanostructures with iron (Fe) [11]. Amongst many other techniques that have been used for synthesizing TNT for DSSCs, DC Anodization is much suitable because of its low cost and simplicity [12,13]. A number of substances have been used as key components of the electrolyte during anodization. In 2009, Sreekantanet al. [14] reported the use of an electrolyte composed of sodium sulfate, ammonium fluoride, sulfuric acid and sodium hydroxide. Later in 2011, Omidvar et al. [15] also reported the use of sulfuric acid and phosphoric acid in an electrolyte composed of deionized (DI) water and ammonium fluoride. In 2012, H. Li et al. [16] successfully used an electrolyte containing DI water, ethylene glycol and ammonium fluoride (NH_4F). This electrolyte composition will be used in this work.

The purpose of this paper is to synthesis Fe-doped TNTs and determine their efficiencies in DSSCs by varying the amount of dopant. The TNTs will be prepared by DC anodization using ethylene glycol and ammonium fluoride electrolyte. The samples will be characterized by X-Ray diffraction (XRD) and scanning electron microscopy (SEM), atomic force microscopy (AFM) and ultraviolet – visible spectrometry (UV-vis) techniques.

Experimental procedure

TiO_2 nanotubes were grown by DC anodization method at 50 V for 2 hours at room temperature. Titanium sheets of 0.25 mm thickness and 99.7 % purity purchased from Sigma Aldrich were first polished with abrasive papers. After polishing, the Ti foils were degreased ultrasonically in isopropanol, deionized water and ethanol. The electrolyte was composed of ethyleneglycol (EG), ammonium fluoride (0.3 wt. % NH_4F), deionized water (2 vol. % D.I. H_2O) and iron (III) nitrate. The concentration of $Fe(NO_3)_3$ was varied from 2, 4, 6 to 10 mM. The electrolyte was kept for 5 hours before anodization to ensure homogeneity. The anodization apparatus is a two-electrode configuration with a piece of highly pure platinum counter electrode.

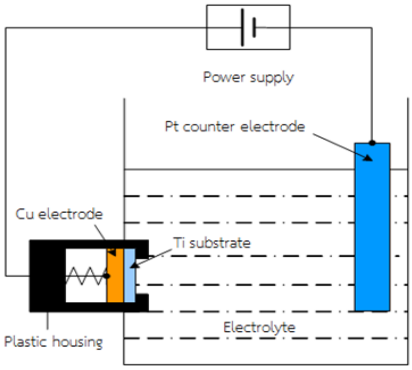

Fig. 1. The schematic diagram of a single-face anodization process

Figure 1 shows the schematic diagram of the anodization process. This set up allows only one face of the Ti foil to be in contact with the electrolyte. Three sets of samples were studied, (a) as anodized without annealing or calcination (b) anodized once and calcinated at 450 °C and (c) re-anodized after calcination at 450 °C. Characterization was done using XRD, SEM, AFM, UV-vis and tested in DSSCs. For the DSSCs, TiO_2 nanotubes photoelectrodes were immersed in 0.5 mM solution of N719 dye in a mixture of acetonitrile/tert-butanol (1:1)

at 25 °C for 24 hours. A transparent conducting oxide (TCO) glass was used as counter electrode. A platinum catalyst was deposited on the TCO glass by coating with drops of platinum solution (H_2PtCl_6). The TCO glass was heated for 30 min at 80 °C. Then, TiO_2 nanotubes photoelectrode and Pt counter electrode were assembled into a sandwich. The TiO_2 nanotubes arrays were finally assembled into DSSCs and their *IV*-characteristics were measured. The photovoltaic properties of the DSSCs were characterized by the four most important parameters, which are the short-circuit current density (J_{sc}), open-circuit voltage (V_{oc}), fill factor (FF) and the conversion efficiency (η). The equations of DSSCs are shown as follows[17]:

$$FF = \frac{V_m I_m}{V_{oc} I_{sc}}, \quad (1)$$

$$\eta = \frac{V_m I_m}{P_{in}} = \frac{V_{oc} I_{sc} FF}{P_{in}}, \quad (2)$$

where I_m and V_m are respectively the current density and voltage at the optimal operationpoint that gives the maximum output power, and P_{in} is the power of the incident light.

Results and discussion

Figure 2 shows the XRD patterns of uncalcinated Fe-doped nanotubes. The peaks at (002), (101), (102), (110), (103) and (112) are characteristic crystal faces of Ti metal. It indicates that the TiO_2 remains in the amorphous phase even for different dopant concentrations. In Fig. 3, the XRD patterns of Fe-doped TNTs annealed at 450 °C are displayed. The diffraction peaks emerging at scattering angles 2θ = 25.3, 48.7, 53.5 and 55.2° correspond to the anatase phase (A). This shows that the crystalline structure of TiO_2 has been transformed from its original amorphous phase after calcination into the anatase phase. These results are in agreement with the work of J.Y. Lin [18].

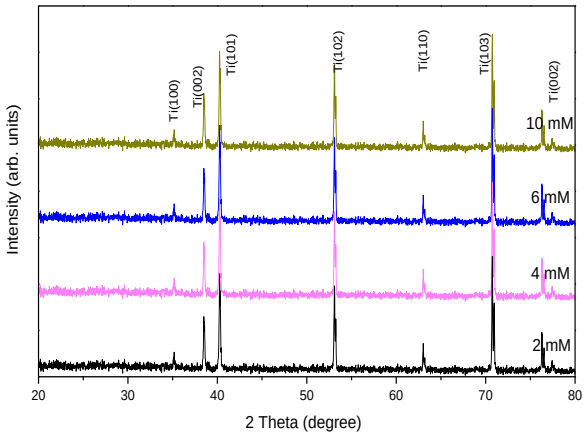

Fig. 2. XRD patterns for Fe-doped TNTs before annealing

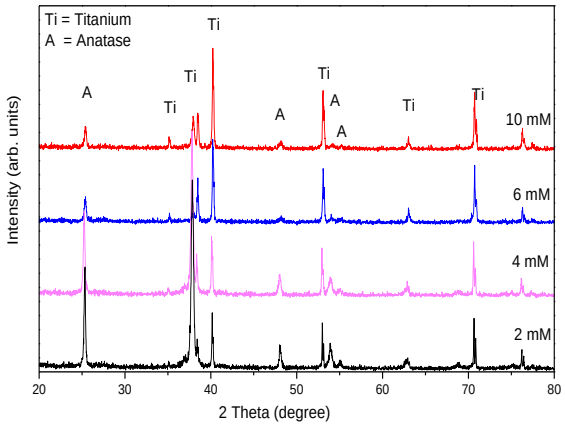

Fig. 3. XRD patterns for Fe-doped TNTs after annealing

The SEM images of the different samples after calcination at 450 °C are shown in Fig. 4. It is observed that as the concentration of dopant substance changes, so too is the surface morphology of the samples. There seems to be an increasing disorder in the array of the nanotubes with increasing dopant concentration. At a-$Fe(NO_3)_3$ concentration of 10 mM, the alignment of the nanotubes are significantly destroyed, as seen in Fig. 4(d). This result is supported by the work of Xiabo Chen et al. [19].

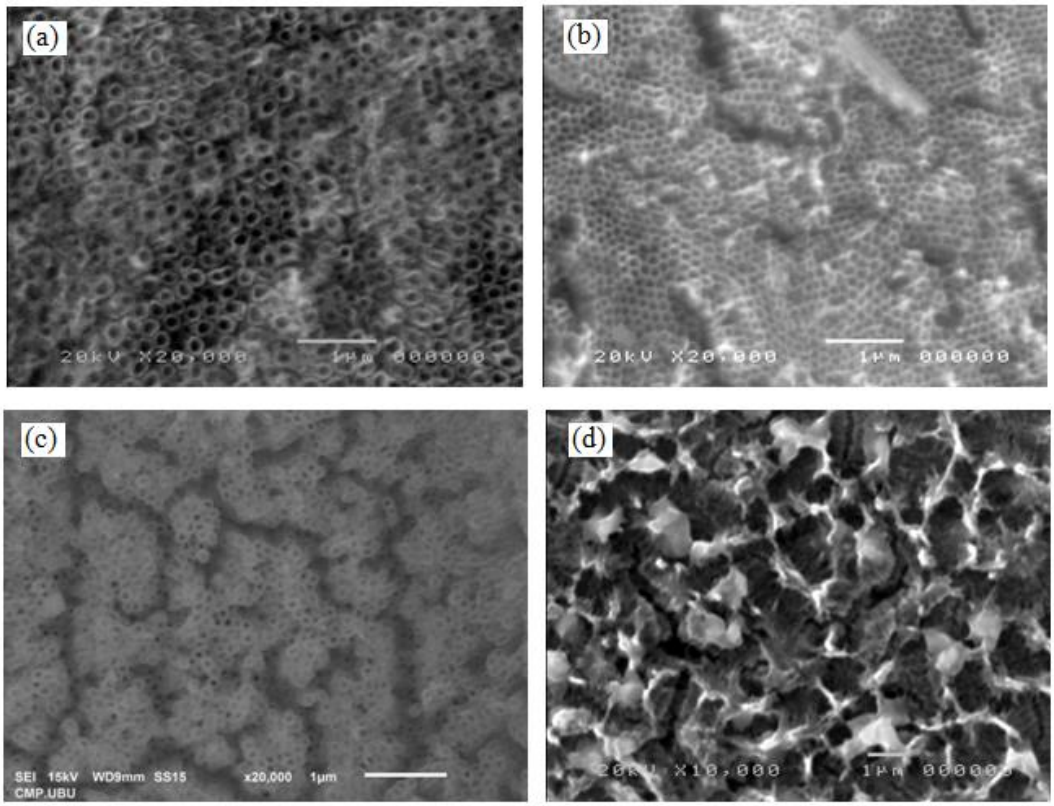

Fig. 4. SEM imagesofFe-doped TNTs with different concentrationsof iron (III) nitrate: (a) 2 mM, (b) 4 mM, (c) 6mM and (d) 10 mM

Could re-anodization after annealing improve the photo-response of the nanotubes? We tried to answer this question by re-anodizing the 6 mM sample, and studied it using SEM, AFM and UV-vis techniques. The SEM image in Fig. 5 shows the surface morphology with lots of cracks and a disordered array of nanotubes. This disorder is also confirmed by the AFM images in Fig. 6. Although the nanotubes appear thicker in diameter, their array is highly non-uniform. The energy band gap of the 6 mM re-anodized sample was determined from the UV-vis spectrum, as shown in Fig. 7. The data at a cut-off wavelength of 388 nm yielded an energy band gap value of 3.20 eV. This value is still as high as that of the pour TiO_2 and would therefore result in a lower efficiency. From the results in Figs. 5-7, we can conclude that it is not recommended to re-anodize the samples after calcinations.

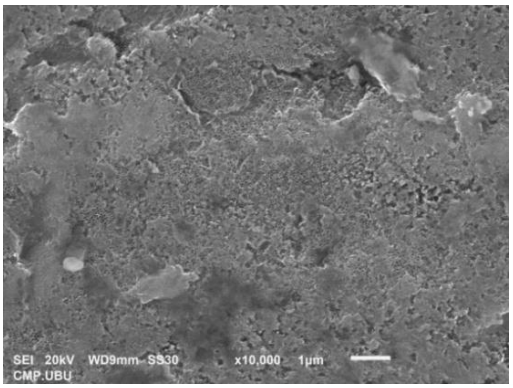

Fig. 5. SEM images of 6 mM sample re-anodized after annealing at 450 °C

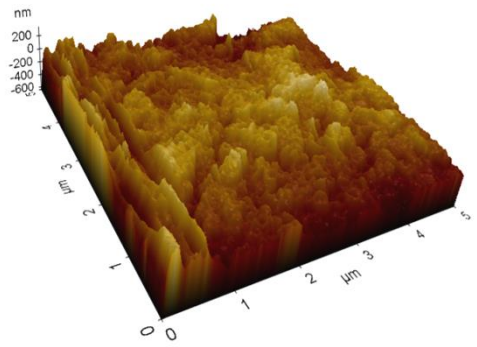

Fig. 6. AFM imagesof 6 mM sample re-anodized after annealing at 450 °C

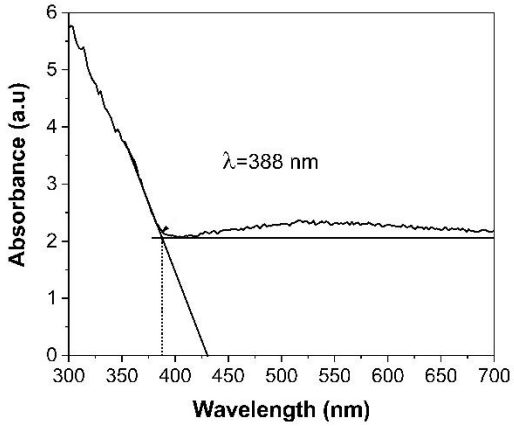

Fig. 7. UV-Visspectrumof 6 mM sample re-anodized after annealing

The IV characteristic in Fig. 8 shows a plot of current density versus voltage, while Table 1 displays the photocatalytic performance of the Fe-doped TNTs in DSSCs. It is observed from both Fig. 8 and Table 1 that as dopant concentration increases, the cell efficiency and photocatalytic performance increases as well. The dopant element, Fe, plays the role of charge traps which hinders charge career recombination. As the concentration of $Fe(NO_3)_3$ increases, more Fe ions displaces Ti ions in the lattice structure. Intermediate energy bands are created, which leads to a lowering of the energy band gap. This results in a shift in optical absorption from the UV region into the visible light spectrum. This is in line with the work of U. Tipparachet al. [20]. The highest cell efficiency of 4.66 % is obtained for a$Fe(NO_3)_3$ concentration of 6 mM. At a higher concentration of 10 mM, the cell efficiency drops dramatically to 2.22 %. As seen from the SEM images in Fig. 4(d), many cracks develop as dopants concentration increases. The arrangement of the nanotubes becomes more disorderly. These conditions lead to more charge carrier recombination and a consequent decrease in photocatalytic performance and cell efficiency.

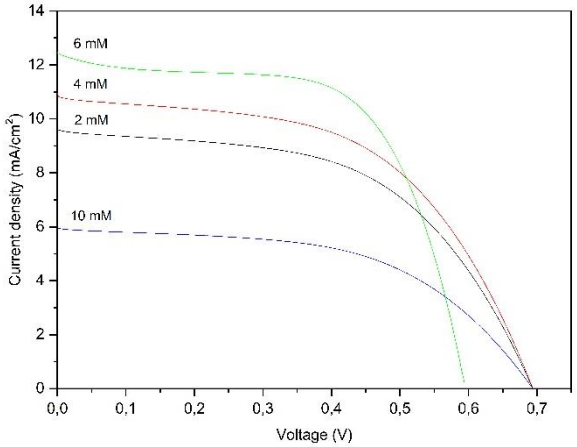

Fig. 8. Current-voltage (IV) characteristic curve of Fe-doped TNTs with varying amounts of $Fe(NO_3)_3$: (a) 2 mM, (b) 4 mM, (c) 6 mM and (d) 10 mM

Table 1. Photocatalytic Performance of Fe-doped TNTs with different concentrations of $Fe(NO_3)_3$

Samples	J_{sc}, mA/cm^2	V_{oc}, V	FF	η, %
2 mM	9.61	0.59	0.63	3.58
4 mM	10.96	0.68	0.54	4.04
6 mM	12.44	0.69	0.56	4.66
10 mM	5.95	0.67	0.50	2.22

Conclusions

In this work, Fe-doped titanium dioxide nanotubes were synthesized by DC anodization using a 50 V supply. The composition of the electrolyte was as follows: ethyleneglycol (EG), ammoniumfluoride (0.3 wt. % NH_4F), deionizedwater (2 vol. % deionizedwater), and $Fe(NO_3)_3$as dopant source with varying concentrations of 2, 4, 6 and 10 mM. The samples were studied before calcination and after calcination at 450 °C. The SEM images were used to study the surface morphology of the samples and revealed the structural arrangement of the nanotubes. The XRD patterns were used to investigate the crystalline phases of Ti and TiO_2. Anatase phases were observed after annealing at 450° C. The photocatalytic performance was studied in DSSCs and showed increased activity with dopant concentration. The highest cell efficiency of 4.66 % was obtained for a$Fe(NO_3)_3$ concentration of 6 mM, after which the cell efficiency dropped. From the results of SEM, AFM and UV-vis studies on the 6 mM sample, we strongly recommend not to re-anodize after annealing, as this does not improve the photo-response of the TNTs. Titanium dioxide nanotubes have a wide range of applications such as in photocatalysis, photovoltaics, hydrogen generation, water purification and fuel cells. The results of this work would serve as a guideline for further research in this field of study.

References

1. Aboulouard A, Gultekin B, Can M, Erol, M, Jouaiti A, Elhadadi B, Demic S. Dye-sensitized solar cells based on titanium dioxide nanoparticles synthesized by flame spray pyrolysis and hydrothermal sol-gel methods: a comparative study on photovoltaic performances. *Journal of Materials Research and Technology*. 2020;9(2): 1569–1577.
2. Shamsudin NH, Shafie S, Ab Kadir MZA, Ahmad F, Sulaiman Y, Chachuli SAM, Razali MC. Flexible back-illuminated dye sensitised solar cells (DSSCs) with titanium dioxide/silver nanoparticles composite photoanode for improvement of power conversion efficiency. *Optik*. 2023;272: 170237.
3. Ahmad I, Jafer R, Abbas SM, Ahmad N, Iqbal J, Bashir S, Khan MH. Improving energy harvesting efficiency of dye sensitized solar cell by using cobalt-rGO co-doped TiO_2 photoanode. *Journal of Alloys and Compounds*. 2022;891: 162040.
4. Gutiérrez Y, Losurdo M, González F, Everitt HO, Moreno F. Nanoplasmonic photothermal heating and near-field enhancements: a comparative survey of 19 metals. *The Journal of Physical Chemistry C*. 2020;124(13): 7386–7395.
5. Joshi DN, Ilaiyaraja P, Sudakar C, Prasath RA. Facile one-pot synthesis of multi-shaped silver nanoparticles with tunable ultra-broadband absorption for efficient light harvesting in dye-sensitized solar cells.*Solar Energy Materials* & *Solar Cells*. 2018;185: 104–110.
6. Jin L, Wang YW, Wu J, Su CY, Zhou H, Xu HY. Properties of oxidation quantum dots-CdO/TiO_2 heterostructures constructed as DSSC photoanodes. *Materials Science in Semiconductor Processing*. 2022;147: 106720.
7. Shaikh SF, Kwon HC, Yang W, Mane RS, Moon J. Performance enhancement of mesoporous TiO_2-based perovskite solar cells by ZnS ultrathin-interfacial modification layer. *Journal of Alloys Compounds*. 2018;738: 405–414.
8. Krasinkova MV. Single-walled carbon nanotube as a nanoscale quantum system. *Materials Physics and Mechanics*. 2020;44: 103–109.
9. Srinivasa Moorthy S, Manonmani K. Fabrication and characterization of TiO_2 particulate filled glass fiber reinforced polymer composite. *Materials Physics and Mechanics*. 2013;13: 28–34.
10. Wang JK, Nie XJ, Wang W, Zhao ZL, Li L, Zhang ZQ. Single-layer graphene-TiO_2 nanotubes array heterojunction as photoanode to enhance the photoelectric of DSSCs. *Optik*. 2021;242: 167245.
11. Ismael M. Enhanced photocatalytic hydrogen production and degradation of organic pollutants from Fe (III) doped TiO_2 nanoparticles. *Journal of Environmental Chemical Engineering*. 2020;8(2): 103676.

12. Chandra Pradhan S, Soman SJ. Effect of thickness on charge transfer properties of conductive polymer based PEDOT counter electrodes in DSSC. *Results in Surfaces and Interfaces*. 2021;5: 100030.
13. Ahmed U, Alizadeh M, Rahim NA, Shahabuddin S, Ahmed MS, Pandey AK. A comprehensive review on counter electrodes for dye sensitized solar cells: A special focus on Pt-TCO free counter electrodes. *Solar Energy*. 2018;174: 1097–1125.
14. Gulati K, Martinez RDO, Czerwiński M, Michalska-Domańska M. Understanding the influence of electrolyte aging in electrochemical anodization of titanium. *Advances in Colloid and Interface Science*. 2022;302; 102615.
15. Yuferov YV, Popov ID, Zykov FM, SuntsovAY, Baklanova IV, ChukinAV, Zhidkov IS. Study of the influence of anodizing parameters on the photocatalytic activity of preferred oriented TiO_2 nanotubes self-doped by carbon. *Applied Surface Science*. 2022;573: 151366.
16. Montakhab E, Rashchi F, Sheibani S. Modification and photocatalytic activity of open channel TiO_2 nanotubes array synthesized by anodization process. *Applied Surface Science*. 2020;534: 147581.
17. Wei X, Wang C, Ding S, Yang K, Tian F, Li F. One-step synthesis of Ag nanoparticles/carbon dots/TiO_2 nanotube arrays composite photocatalyst with enhanced photocatalytic activity. *Journal of Environmental Chemical Engineering*. 2021;9(1): 104729.
18. Motola M, Hromadko L, Prikryl J, Sopha H, Krbal M, Macak JM. Intrinsic properties of high-aspect ratio single-and double-wall anodic TiO_2 nanotube layers annealed at different temperatures. *Electrochimica Acta*. 2020;352: 136479.
19. Nakpan P, Aeimbhu A. Fabrication of titanium dioxide nanotubes by difference the anodization voltage and time. *Materials Today: Proceedings*. 2021;47: 3436–3440.
20. Purushothaman N, Elansezhian R, Raviprakash AV. Synthesis and characterisation of nano TiO_2 film for enhancing antireflection properties. *Advances in Materials and Processing Technologies*. 2022;8(1): 29–36.

THE AUTHORS

Samran B.
e-mail: buagun@hotmail.com

Timah E.N.
e-mail: timahe@yahoo.com

Thongpanit P.
e-mail: p.thongpanit@npu.ac.th

Chaiwichian S.
e-mail: saranyou530531117@gmail.com